Soil Biology & Biochemistry 44 (2012) 102–112

Contents lists available at SciVerse ScienceDirect

Soil Biology & Biochemistry

journal homepage: www.elsevier.com/locate/soilbio

Spatial variation of soil $\delta^{13}C$ and its relation to carbon input and soil texture in a subtropical lowland woodland

Edith Bai [a,*], Thomas W. Boutton [b], Feng Liu [b], X. Ben Wu [b], C. Thomas Hallmark [c], Steven R. Archer [d]

[a] State Key Laboratory of Forest and Soil Ecology, Institute of Applied Ecology, Chinese Academy of Sciences, Shenyang, Liaoning 110164, China
[b] Department of Ecosystem Science and Management, Texas A&M University, College Station, TX 77843-2138, USA
[c] Department of Soil and Crop Sciences, Texas A&M University, College Station, TX 77843-2474, USA
[d] School of Natural Resources and the Environment, University of Arizona, Tucson, AZ 85721-0043, USA

ARTICLE INFO

Article history:
Received 29 November 2010
Received in revised form
15 September 2011
Accepted 17 September 2011
Available online 11 October 2011

Keywords:
Stable carbon isotopes
Woody plant encroachment
Soil texture
Soil organic carbon

ABSTRACT

Spatial patterns of soil $\delta^{13}C$ were quantified in a subtropical C_3 woodland in the Rio Grande Plains of southern Texas, USA that developed during the past 100 yrs on a lowland site that was once C_4 grassland. A 50 × 30 m plot and two transects were established, and soil cores (0–15 cm, $n = 207$) were collected, spatially referenced, and analyzed for $\delta^{13}C$, soil organic carbon (SOC), and soil particle size distribution. Cross-variogram analysis indicated that SOC remaining from the past C_4 grassland community co-varied with soil texture over a distance of 23.7 m. In contrast, newer SOC derived from C_3 woody plants was spatially correlated with root biomass within a range of 7.1 m. Although mesquite trees initiate grassland-to-woodland succession and create well-defined islands of soil modification in adjoining upland areas at this site, direct gradient and proximity analyses accounting for the number, size, and distance of mesquite plants in the vicinity of soil sample points failed to reveal any relationship between mesquite tree abundance and soil properties. Variogram analysis further indicated soil $\delta^{13}C$, texture and organic carbon content were spatially autocorrelated over distances (ranges = 15.6, 16.2 and 18.7 m, respectively) far greater than that of individual tree canopy diameters in these lowland communities. Cross-variogram analysis also revealed that $\delta^{13}C$ – SOC and $\delta^{13}C$-texture relationships were spatially structured at distances much greater than that of mesquite canopies (range = 17.6 and 16.5 m, respectively). These results suggest fundamental differences in the functional nature and consequences of shrub encroachment between upland and lowland landscapes and challenge us to identify the earth system processes and ecosystem structures that are driving carbon cycling at these contrasting scales. Improvements in our understanding how controls over soil carbon cycling change with spatial scale will enhance our ability to design vegetation and soil sampling schemes; and to more effectively use soil $\delta^{13}C$ as a tool to infer vegetation and soil organic carbon dynamics in ecosystems where C_3–C_4 transitions and changes in structure and function are occurring.

1. Introduction

Natural stable isotope ratios are widely used in ecological research as intrinsic tracers to investigate structural and functional characteristics of ecosystems and their responses to environmental changes and human activities (Amundson et al., 1998; Boutton et al., 1999; Ehleringer et al., 2000; Pataki et al., 2003, 2007; West et al., 2010). Soil carbon isotopic signatures ($\delta^{13}C$) are commonly used to reconstruct plant community history, determine sources of soil organic carbon (SOC), and quantify SOC turnover rates (Balesdent et al., 1987; Choi et al., 2001; Sanaiotti et al., 2002; Krull et al., 2007; Boutton et al., 2009a). Soil $\delta^{13}C$ values correspond closely to the $\delta^{13}C$ of plant residues entering the system through litterfall and root turnover (Nissenbaum and Schallinger, 1974; Ludlow et al., 1976; van Kessel et al., 1994). After plant residues enter the soil, their $\delta^{13}C$ values may be modified slightly from their initial value by isotope fractionation associated with microbial decay processes, and by differential decay of isotopically unique biochemical compounds that comprise soil organic matter (Blair et al., 1985; Agren et al., 1996; Santruckova et al., 2000; Fernandez et al., 2003; Crow et al., 2006). Therefore, variation in soil $\delta^{13}C$ values and their evolution over time are controlled primarily by carbon inputs from vegetation and secondarily by biological decay processes (Nadelhoffer and Fry, 1988; Garten et al.,

* Corresponding author. Tel.: +86 24 83970570.
E-mail address: baie@iae.ac.cn (E. Bai).

0038-0717/$ – see front matter © 2011 Elsevier Ltd. All rights reserved.
doi:10.1016/j.soilbio.2011.09.013

2000). Here we examined the influence of these two processes on the spatial pattern of soil $\delta^{13}C$ on a site transformed from grasslands dominated by C_4 plants to woodlands dominated by a C_3 plants.

At ecosystem to global scales the relative abundance of C_3 and C_4 plants exerts the strongest control over soil $\delta^{13}C$. $\delta^{13}C$ values of C_3 plants range from −32 to −22‰, while those with C_4 photosynthesis range from −17 to −9‰ (Farquhar et al., 1989), with the $\delta^{13}C$ of SOC usually reflecting the magnitude of C_3 and C_4 plant inputs to community net primary productivity (Troughton et al., 1974; Balesdent and Mariotti, 1996; Suits et al., 2005). In areas where vegetation has changed from one photosynthetic pathway type to another (e.g., $C_4 \rightarrow C_3$, or vice versa), SOC reflects a combination of inputs from both the past vegetation and the current vegetation, the isotopic signal from the original vegetation persisting in the SOC pool for a duration dependent on the turnover rate of SOC in that ecosystem. Soil $\delta^{13}C$ values have thus been utilized to document vegetation changes in a variety of ecosystem types around the world where plant cover has changed from C_4 to C_3 or vice versa (Boutton, 1996; Krull et al., 2005; Dümig et al., 2008; Silva et al., 2008; Wittmer et al., 2009). In this study a geostatistical analysis of spatial patterns of soil $\delta^{13}C$ was undertaken as a means of assessing how the development of C_3 woodland communities on C_4 grasslands has influenced soil carbon pools.

Organic matter inputs from C_3 vs. C_4 plants are modified during the decomposition process to influence soil $\delta^{13}C$ (Boutton et al., 1998; Liao et al., 2006a; Wynn and Bird, 2007; Diochon and Kellman, 2008). For example, soil factors that retard decomposition rates will favor the persistence of carbon derived from the original C_4 vegetation and hence affect soil $\delta^{13}C$ values (Balesdent et al., 1987; Desjardins et al., 1994; Balesdent and Mariotti, 1996; Bird et al., 2003; Liao et al., 2006a). Under similar climatic conditions, the dominant factor controlling decomposition processes is soil texture (Schimel et al., 1994; Jobbagy and Jackson, 2000), with slower rates of SOC turnover in fine-textured soils where clay micelles protect organic matter from mineralization (Anderson and Paul, 1984; Feller and Beare, 1997; Hassink, 1997). It is therefore important to understand and account for the influences of soil texture on soil $\delta^{13}C$ to effectively use soil carbon isotope techniques to study vegetation change and soil carbon cycling processes. Here, we use omnidirectional variogram analyses to quantify the spatial scale of variation in soil $\delta^{13}C$, SOC and texture; and cross-variogram analyses to determine the spatial scale over which variation in soil $\delta^{13}C$ values are correlated with SOC pools and soil texture. We then relate the scales of spatial variation in soil $\delta^{13}C$, SOC and texture to present-day patterns in vegetation distribution.

The simultaneous application of geostatistical approaches with isotopic analyses of the plant-soil system promises to be a powerful approach for interpreting ecosystem and ecological processes at landscape and regional scales (e.g., van Kessel et al., 1994; Marriott et al., 1997; Biggs et al., 2002; Boeckx et al., 2006; Powers, 2006; West et al., 2010). Despite the potential for understanding and quantifying ecosystem processes such as soil carbon dynamics and vegetation change at the landscape scale, the union of these methodologies remains largely unexplored. Here we combined these approaches to quantify the spatial scaling of soil isotopic values and identify the factors controlling it.

In the Rio Grande Plains of southern Texas, subtropical thorn woodlands dominated by C_3 honey mesquite (*Prosopis glandulosa*) trees have become significant components of landscapes once dominated almost exclusively by C_4 grasslands (Archer et al., 1988; Boutton et al., 1998). In the sandy loam upland portions of the landscape, this grassland-to-woodland conversion is initiated when a mesquite tree establishes within the grassland and then facilitates the establishment of other woody species beneath its canopy (Archer et al., 1988), resulting in the formation of discrete shrub islands within a grassland matrix. Recent studies have confirmed this pattern of woody patch development, and showed that the scale of variation in soil $\delta^{13}C$ in the upland were tightly coupled to discrete patterns of shrub distribution but not to scales of soil clay distribution (Bai et al., 2009). With this study we sought to extend our isotopic assessment of upland successional processes to adjoining lowlands characterized by a woodland physiognomy.

Given that these lowland woodlands are characterized by a mesquite overstory with an understory shrub species composition generally similar to that of upland woody patches, our working hypothesis is that grassland-to-shrubland successional processes similar to those operating in uplands have also occurred in these low-lying portions of the landscape (Archer, 1995). If this hypothesis is correct, then we would expect to see patterns of soil $\delta^{13}C$ that vary in accordance with patterns of mesquite distribution. To test this hypothesis, we sought to: (1) determine spatial scale of variation of soil $\delta^{13}C$ in a C_3 woodland formerly dominated by C_4 grasses; (2) examine spatial relationships between soil $\delta^{13}C$, SOC pools and soil texture; and (3) investigate spatial correlations between soil $\delta^{13}C$ and the relative proportions of SOC derived from C_3 vs. C_4 plant sources. In contrast to uplands, we found that the scale of pattern in soil $\delta^{13}C$ in lowlands substantially exceeded that of mesquite plant canopies. These results suggest the mesquite overstory is no longer the dominant source of SOC; that translocation of surface litter and sediments by intermittent flooding has obscured local plant-induced gradients; or that grassland-to-woodland succession has occurred via different mechanisms on this landform.

2. Materials and methods

2.1. Study area

Research was conducted at the Texas AgriLife La Copita Research Area in Jim Wells County, 15 km SW of Alice, TX (27° 40′ N; 98° 12′ W) in the eastern Rio Grande Plains of the Tamaulipan Biotic Province. The climate is subtropical with a mean annual temperature of 22.4 °C. Mean annual precipitation is 680 mm with bimodal maxima in May–June and September.

La Copita landscapes grade (1–3% slopes) from sandy loam uplands (approximately 85–90 m asl) to clay loam lowlands (approximately 84–85 m asl) that receive runoff from the uplands (Wu and Archer, 2005) and have intermittent water flow during high rainfall periods. This study was conducted in the lowland portion of the landscape, characterized by closed-canopy woodlands dominated by honey mesquite and lime prickly ash (*Zanthoxylum fagara* (L.) Sarg.). Soils in the lowlands are finer-textured clay loams (Pachic Argiustolls), with pH ranging from 4.4 to 7.7. Woody plant encroachment in the study area over the past 75–100 years due to the interaction of livestock grazing and reduced fire frequency has been well documented (Archer, 1995; Archer et al., 2001).

2.2. Study design and field sampling

A 50 × 30 m plot consisting of 5 × 5 m grid cells was established in 2004 (Fig. 1). This specific location was chosen because it allowed us to install a plot with relatively large dimensions entirely within a drainage woodland landscape that has been free from human disturbance (except for low to moderate levels of livestock grazing) since at least 1930. The corners of the plot were georeferenced using a high resolution GPS (Trimble Pathfinder Pro XRS, Trimble Navigation Ltd, Sunnyvale, CA). The locations of cell corners and transect points within the grid were calculated based on measured distances to the georeferenced points. Locations of all mature

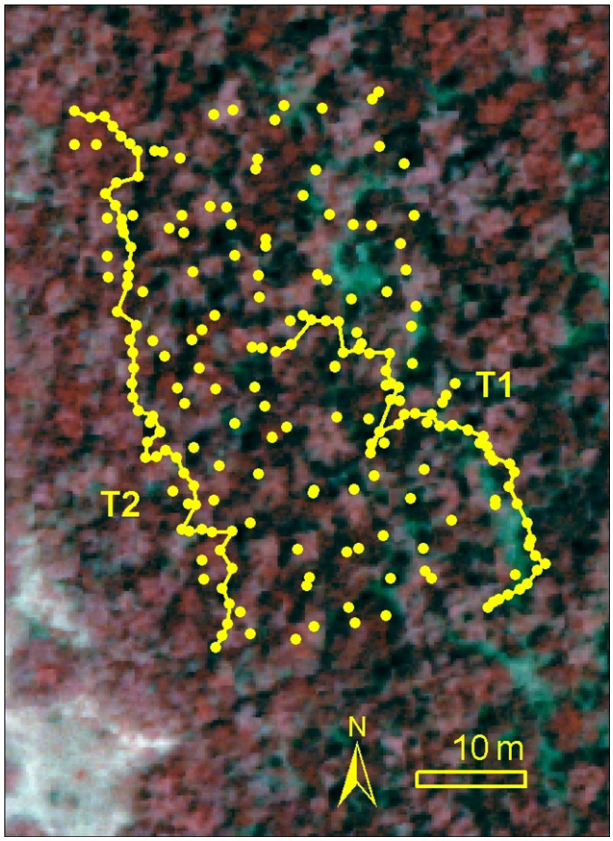

Fig. 1. Aerial view of the intermittent drainage woodland study area in southern Texas, USA. Darker red area represents woody vegetation canopies. Yellow dots represent soil sampling points within a grid comprised of 5 × 5 m cells; and along two transects (T1, T2). T1 generally followed the topographic low of the intermittent drainage; and T2 was upslope about half-way between the topographic low and the upland/lowland interface defined by the woodland margin. (For interpretation of the references to color in this figure legend, the reader is referred to the web version of this article.)

mesquite trees (basal diameter > 5 cm) within the plot were mapped and their basal diameters recorded.

Two points were randomly selected for sampling within each grid cell and their locations mapped. In addition, two tree-to-tree transects at the two parallel edges of the grid, each about 70 m in length, were established (Fig. 1). Transect 1 (T1) generally followed the topographic low of the intermittent drainage; and Transect 2 (T2) was upslope about half-way between the topographic low and the upland/lowland interface defined by the woodland margin. These transects zigzagged from one mesquite tree to the next in a generally north-south orientation. Basal diameter was measured for each mesquite plant; soil samples were categorized to three classes: "base" indicates points adjacent to mesquite tree trunks; "edge" indicates points on the dripline of the tree canopy; and "mid" indicates points between the canopy edge and the base. There were 41 and 47 sampling points for the T1 and T2, respectively. At each sampling point in the grid and along the transects, three soil cores (15 cm deep × 2.24 cm in diameter) were collected. Distances from the soil sampling points to the nearest mesquite tree were calculated using ArcView GIS Spatial Analyst (ESRI, 1998). Sampling was limited to the upper 15 cm of the profile because our previous studies have indicated that changes in root biomass, SOC, and soil $\delta^{13}C$ following woody encroachment are most pronounced in this depth interval (Boutton et al., 2009a).

It should be noted that soil corers <3.8 cm in diameter provide lower estimates of root biomass than larger diameter corers (Ping et al., 2010). However, larger diameter corers yield amounts of soil that are more difficult to mix and homogenize thoroughly during sample preparation, and there is greater potential for random sampling error when taking a mg-sized aliquot for elemental and/or isotopic analysis (Brown, 1999).

2.3. Soil analysis

One of the three soil cores collected at each sample point was used for determination of root biomass using a hydropneumatic elutriation system (Gillison's Variety Fabrications Inc., Benzonia, MI, USA) (Smucker et al., 1982) with 410 μm filters. Roots were dried for at least 72 h at 60 °C to determine dry weight, and then ashed at 400 °C in a muffle furnace to obtain ash-free root biomass.

The second soil core was used for bulk density and soil particle size analysis. Soil bulk density was determined by the core method (Soil Survey Staff, 1996). Organic fragments and gravel >2 mm were removed by sieving, and aggregates were crushed by hand, however, the volume that the <2 mm fraction occupies was not adjusted in bulk density calculations. Particle size distribution was determined by the pipette method (Gee and Bauder, 1986). All results of particle size analysis are expressed as the percentage, by weight, of the oven-dried soil.

The third soil core was used for pH, elemental and isotopic analysis. Soils were passed through a 2 mm sieve to remove coarse organic fragments and gravel. An aliquot of soil (10 g) was analyzed for pH in 0.01 M $CaCl_2$ (Accumet Basic pH meter, Fisher Scientific, Pittsburgh, PA). The remainder of the soil was dried at 60 °C for 48 h, and ground in a centrifugal mill (Angstrom, Inc., Belleville, MI). Soil samples were weighed into silver capsules, treated with HCl vapor in a desiccator (Harris et al., 2001) to volatilize inorganic carbon, and analyzed for SOC and $\delta^{13}C$ of SOC using a Carlo Erba EA-1108 elemental analyzer interfaced with a Delta Plus continuous flow isotope ratio mass spectrometer (ThermoFinnigan, San Jose, CA). Total N was determined in the same manner but without pretreatment with HCl vapor.

Carbon isotope ratios are presented in standard δ notation (Coplen, 1996). Precision of duplicate measurements was 0.1‰ for $\delta^{13}C$.

The proportion of carbon derived from grassland was estimated by the mass balance equation:

$$\delta^{13}C_{SOM} = \left(\delta^{13}C_G\right)(f_G) + \left(\delta^{13}C_W\right)(1 - f_G) \quad (1)$$

where $\delta^{13}C_{SOM}$ is the $\delta^{13}C$ value of the whole soil organic matter, $\delta^{13}C_G$ is the average $\delta^{13}C$ value of the original grassland, f_G is the proportion of carbon from grassland sources, $\delta^{13}C_W$ is the average $\delta^{13}C$ value of the woody components, and $(1 - f_G)$ is equal to the proportion of carbon derived from woody plant sources. In this study, we used −16.5‰ as $\delta^{13}C_G$ and −26‰ as $\delta^{13}C_W$ based on previous studies in the same area (Bai et al., 2008, 2009).

The content of carbon derived from the new woody input (C_W) and that remaining from previous grassland (C_G) was calculated as:

$$C_W = C_T \times (1 - f_G) \quad (2)$$

$$C_G = C_T \times f_G \quad (3)$$

where C_T is the total soil organic carbon concentration (g C kg^{-1} soil).

2.4. Mesquite influence index

To determine if grassland-to-woodland succession in the lowlands is first initiated by the establishment of mesquite trees,

we evaluated whether or not spatial patterns of SOC and soil $\delta^{13}C$ were related to the distribution of mesquite trees throughout the study site. Ghazoul et al. (1998) used a proximity index to measure the relative isolation of flowering trees to a focal tree to study the effect of cross-pollination on reproductive success of bees. Based on this idea, in order to estimate the influence of mesquite trees on soil properties, we define a generalized proximity index (GPI):

$$\mathrm{GPI} = \sum_{i=1}^{n} D_i/Z_i \tag{4}$$

where Z_i is the distance in meters from the soil sampling point to each surrounding mesquite within a 12 m diameter circle (for points immediately adjacent to a mesquite tree, a $Z_i = 0.001$ was assigned (instead of using $Z_i = 0$) for calculation), and D_i is the basal diameter of the mesquite in meters. Therefore, this index considers the number, size, and distance to conspecific neighbors within a range, weighted in favor of the nearest and largest individuals. GPI is larger when the soil sampling point is surrounded by nearer, more, and/or larger mesquite, and decreases as mesquite become further, sparser, and/or smaller.

2.5. Spatial and statistical analyses

Descriptive statistics were computed with SPSS for Windows, version 11.5 (SPSS Inc., Chicago, IL, 2002). Spatial ANOVA (SpaceStat, Ann Arbor, MI, 2000) was used to compare the means of soil properties of different transects (T1 and T2) and transect sampling positions (mesquite base, mid-canopy, and canopy edge). For the spatial ANOVA, autocorrelations were evaluated within the range determined from semivariogram analyses (Goovaerts, 1997). Pearson's correlation coefficients and a modified *T*-test for correlation were calculated to test for correlations between soil $\delta^{13}C$, GPI, root biomass, SOC pools, and soil particle size distribution for the entire data set (grid plus transects). The modified *T*-test adjusts the degrees of freedom based on the extent of spatial autocorrelation in the data, therefore compensates for spatial autocorrelation (Clifford et al., 1989; Dutilleul et al., 1993). The software used was PASSAGE version 1 (Rosenberg, 2001).

Semivariogram analysis (Goovaerts, 1997) was used to determine the spatial autocorrelation pattern for soil properties using VARIOWIN (Pannatier, 1996). The experimental semivariance (γ) for the lag distance h was calculated as:

$$\gamma(h) = \frac{1}{2N(h)} \sum_{i=1}^{i=N(h)} \left[Z(x_i) - Z(x_{i+h})\right]^2 \tag{5}$$

where $Z(x_i)$ and $Z(x_{i+h})$ are the values of measured properties at spatial location x_i and x_{i+h}, and $N(h)$ is the number of pairs with lag distance h. Ordinary kriging was used as a spatial interpolation tool for predicting values at unsampled locations based on sample data and the spatial structure of the sample data determined using variogram analysis.

Cross-semivariogram analysis (Rossi et al., 1996; Goovaerts, 1997) was used to determine the spatial correlation between soil $\delta^{13}C$ and soil properties:

$$\gamma(h) = \frac{1}{2N(h)} \sum_{i=1}^{i=N(h)} \left[Z(x_i) - Z(x_{i+h})\right] \times \left[Y(x_i) - Y(x_{i+h})\right] \tag{6}$$

where $Z(x_i)$ and $Z(x_{i+h})$ are the values of the primary variable (e.g. soil $\delta^{13}C$ in our study) and $Z(x_i)$ and $Z(x_{i+h})$ are the values of the secondary variable (e.g. silt + clay content in our study) at spatial location x_i and x_{i+h}. Other parameters are as defined for semivariogram analysis. The proportion of the sill explained by spatial dependence ($\mathrm{Sill}_{(SD)}$), which indicates the spatial structure at the sampling scale was computed as:

$$\mathrm{Sill}_{(SD)}(\%) = [(\mathrm{sill} - \mathrm{nugget})/\mathrm{sill}] \times 100 \tag{7}$$

3. Results

3.1. Soil chemical and physical properties

Based on the entire data set (all grid and transect samples combined), coefficients of variation for soil chemical and physical properties ranged from 8% for soil $\delta^{13}C$ values to 58% for root biomass density (Table 1). Soil $\delta^{13}C$ values varied by approximately 8‰ and revealed that SOC was almost entirely derived from C_4 plants in some portions of this woodland ($\delta^{13}C = -16.2$‰), but almost entirely C_3-derived in others ($\delta^{13}C = -23.8$‰).

Soil $\delta^{13}C$ averaged −19.4‰ along the topographic low transect (T1) and −20.3‰ along the upslope transect (T2) (Table 2). Soil texture did not differ between the two transects. However, SOC, TN, pH, BD and root biomass all showed significant differences between the two transects. Soil chemical and physical properties were not affected by GPI.

3.2. Spatial patterns of soil properties

Results of semivariogram analyses are summarized in Table 3. Values for soil $\delta^{13}C$, C_T, C_G, and silt + clay content derived from the grid points had spatial autocorrelation ranges of 15.6 m, 18.7 m, 17.6 m, and 16.2 m, respectively, and were very different from that of root biomass (4.3 m) and C_W (50.0 m). The proportion of the sill explained by spatial dependence (Eq. (7)), which indicates the spatial structure at the sampling scale, ranged from 29.4% for root biomass to 77.8% for C_G.

Kriged maps developed from the grid points revealed that soil $\delta^{13}C$ (Fig. 2a) and silt + clay content (Fig. 2b) were typically highest in the topographic low region in the center of the plot, gradually increasing upslope toward the east and west. Patterns of C_G and C_W

Table 1
Descriptive statistics for soil chemical and physical properties (0–15 cm) within an intermittent drainage characterized by a C_4 woodland that has replaced a C_4 grassland. All the sample points in the grids and transects are included ($n = 207$).

	Organic carbon (g C kg^{-1})	Total nitrogen (g N kg^{-1})	pH	Bulk density (g cm^{-3})	$\delta^{13}C$ (‰)	Root biomass (g m^{-2})	Soil texture (%)		
							Sand	Silt	Clay
Mean	19.3	1.67	6.15	1.11	−19.46	728.6	56.4	20.9	22.7
Minimum	9.3	0.70	4.37	0.75	−23.83	144.4	40.2	14.7	13.5
Maximum	46.1	4.50	7.67	1.39	−16.24	2014.5	71.8	32.4	39.8
Standard deviation	6.2	0.62	0.79	0.14	1.51	363.2	6.6	3.2	4.8
Skewness	0.9	1.24	−0.08	−0.28	−0.26	1.6	−0.1	0.8	0.6
Coefficients of variation	33%	37%	13%	13%	8%	50%	12%	15%	21%

Table 2
Comparison of soil chemical and physical properties along the transects within an intermittent drainage characterized by a C_3 woodland that has replaced a C_4 grassland. Transect 1 (T1) generally followed the topographic low of the intermittent drainage; and Transect 2 (T2) was upslope about half-way between the topographic low and the upland/lowland interface defined by the woodland margin. "Base" indicates points adjacent to mesquite tree trunks; "edge" indicates points on the dripline of the tree canopy; and "mid" indicates points between the canopy edge and the base. Different superscript letters represent significant difference between the means tested by spatial ANOVA ($p = 0.01$).

	Organic carbon (g C kg^{-1})	Total nitrogen (g N kg^{-1})	pH	Bulk density (g cm^{-3})	δ^{13}C (‰)	Root biomass (g m^{-2})	Soil texture (%)			
							Sand	Silt	Clay	Silt + Clay
T1	15.8^a	1.37^a	5.8^a	1.16^a	−19.4^a	679.0^a	59.3^a	21.2^a	19.5^a	40.7^a
T2	22.6^b	2.05^b	6.7^b	1.07^b	−20.3^b	1162.1^a	57.8^a	19.5^a	22.7^a	42.2^a
Base	19.9^a	1.77^a	6.0^a	1.08^a	−20.1^a	966.9^a	60.1^a	20.0^a	20.0^a	40.0^a
Mid	20.7^a	1.86^a	6.3^a	1.09^a	−20.2^a	1147.8^a	58.4^a	20.2^a	21.4^a	41.6^a
Edge	17.5^a	1.53^a	6.3^a	1.16^a	−19.4^a	775.6^a	57.7^a	20.7^a	21.6^a	42.3^a

also appeared to vary along these subtle elevation gradients, with C_G decreasing and C_W increasing away from the plot center (Fig. 2c and d).

3.3. Correlation between soil δ^{13}C and proximity of mesquite trees

Modified *T*-tests corrected for spatial autocorrelation and Pearson's correlation coefficients showed no evidence that GPI of mesquite trees was correlated with soil δ^{13}C from the grid samples ($r = -0.12$; $p > 0.05$) (Table 4). The null relationship between GPI and root biomass also confirmed the lack of effects of mesquite trees on belowground properties. Furthermore, δ^{13}C values of soils obtained at the base, and canopy edge of mesquite trees were comparable; and values along the two transects showed no evidence that soil δ^{13}C values were consistently influenced by the presence of mesquite trees based on ANOVA analysis (Fig. 3a and b; Table 2).

3.4. Correlation between soil δ^{13}C, soil texture, root biomass, and SOC

Soil δ^{13}C was significantly and negatively correlated with root biomass density ($r = -0.48$; $p < 0.01$) and total SOC concentration ($r = -0.63$; $p < 0.01$) based on grid data points (Table 4). Soil δ^{13}C was positively correlated with soil silt + clay content ($r = 0.41$; $p < 0.01$) and negatively correlated with sand content ($r = -0.41$; $p < 0.01$) (Table 4). The concentration of SOC derived from the previous C_4 grassland (C_G) consistently increased with increases in soil silt + clay content (Fig. 4a), whereas the concentration of SOC derived from the more recently established C_3 woody plants (C_W) varied independently of this parameter (Fig. 4b).

Table 3
Spatial patterns of soil properties (0–15 cm) within the woodland sampling grid. (a) Omnidirectional variogram of soil δ^{13}C (‰); SOC concentration (g C kg^{-1}) in total soil (C_T); and soil silt + clay (%), SOC derived from previous grassland (C_G), SOC derived from new woody input (C_W) and root biomass (g m^{-2}). (b) Cross-variograms assessing potential spatial correlations.

	Nugget	Sill	Range (m)	(Sill − Nugget)/Sill (Eq. (7); %)
(a) *Omnidirectional variograms*				
Soil δ^{13}C	1.1	2.4	15.6	51.3
C_T	13.8	39.3	18.7	64.9
C_W	21.8	31.9	50.0	31.7
Root biomass	95797.3	135734.6	4.3	29.4
C_G	3.0	13.5	17.6	77.8
Silt + clay	18.5	58.8	16.2	68.5
(b) *Cross-variograms*				
Soil δ^{13}C − C_T	−2.9	−5.6	17.6	48.2
Soil δ^{13}C − Silt + clay	0.5	5.1	16.5	91.1
C_W − Root biomass	130.2	785.4	7.1	83.4
C_G − Silt + clay	3.5	24.5	23.7	85.7

Modeled cross-variogram results are summarized in Table 3. Soil δ^{13}C and SOC concentration based on grid data points showed that the two variables were negatively correlated spatially (nugget = −2.9; sill = −5.6) over a distance of 17.6 m. Soil δ^{13}C and silt + clay content were positively spatially correlated (nugget = 0.5, sill = 5.1) over a range of 16.5 m and their spatial dependence ($Sill_{(SD)}$) was 91%. C_W was spatially correlated with root biomass (nugget = 130.2, sill = 785.4) within 7.1 m and C_G was spatially correlated with silt + clay (nugget = 3.5, sill = 24.5) within 23.7 m.

From visual inspection of the kriged maps developed from the sample grid data points (Fig. 2a–d), it is apparent that areas with higher soil δ^{13}C values were associated with the occurrence of higher silt + clay content, higher C_G and lower C_W (e.g., central grid area).

4. Discussion

4.1. Spatial pattern of soil δ^{13}C

Historical aerial photos, tree rings, simulation models, and soil δ^{13}C values have all confirmed that woody plant invasion occurred throughout the study area over the past 100 years (Boutton et al., 1998; Archer et al., 2001). Although upland areas still have a parkland configuration comprised of discrete woody patches within a grassland matrix, woodlands have completely replaced grasslands in the lower-lying portions of this landscape. Soil δ^{13}C values in these lowland woodlands were variable and ranged from −23.8‰ to −16.2‰ (average = −19.5‰) (Table 1). These soil δ^{13}C values were higher than those of surface litter (−28 to −26‰) and the leaves of mesquite (−26 to −25‰) (Boutton et al., 1998; Bai et al., 2008). This demonstrates that although the current woodland vegetation in lowlands is dominated exclusively by C_3 trees and shrubs, the soil retains a strong isotopic memory of the C_4 grasslands that once occupied this area. This is entirely consistent with previous studies in the area (Archer, 1995; Boutton et al., 1998, 1999; Archer et al., 2001; Boutton et al., 2009a).

Despite the relatively uniform and continuous C_3 woody plant cover in the study area (Fig. 1), the spatial pattern of soil δ^{13}C was surprisingly heterogeneous (Table 3, Fig. 2a). The scale of the measurements was approximately 1 m. Semivariogram analysis indicated that autocorrelation accounted for 51.3% of the variability and that soil δ^{13}C values were no longer autocorrelated at distances >15.6 m (nugget = 1.13, sill = 2.36, range = 15.6) (Table 3). Numerous factors have the potential to contribute to the scale of variation in soil δ^{13}C including (a) spatial variation in plant community composition (e.g., the local occurrence of C_4 grasses in shrub canopy gaps), (b) interspecific differences in δ^{13}C values of the numerous shrub and herb species comprising these woodlands, (c) above- vs. belowground carbon allocation patterns, (d) rates of

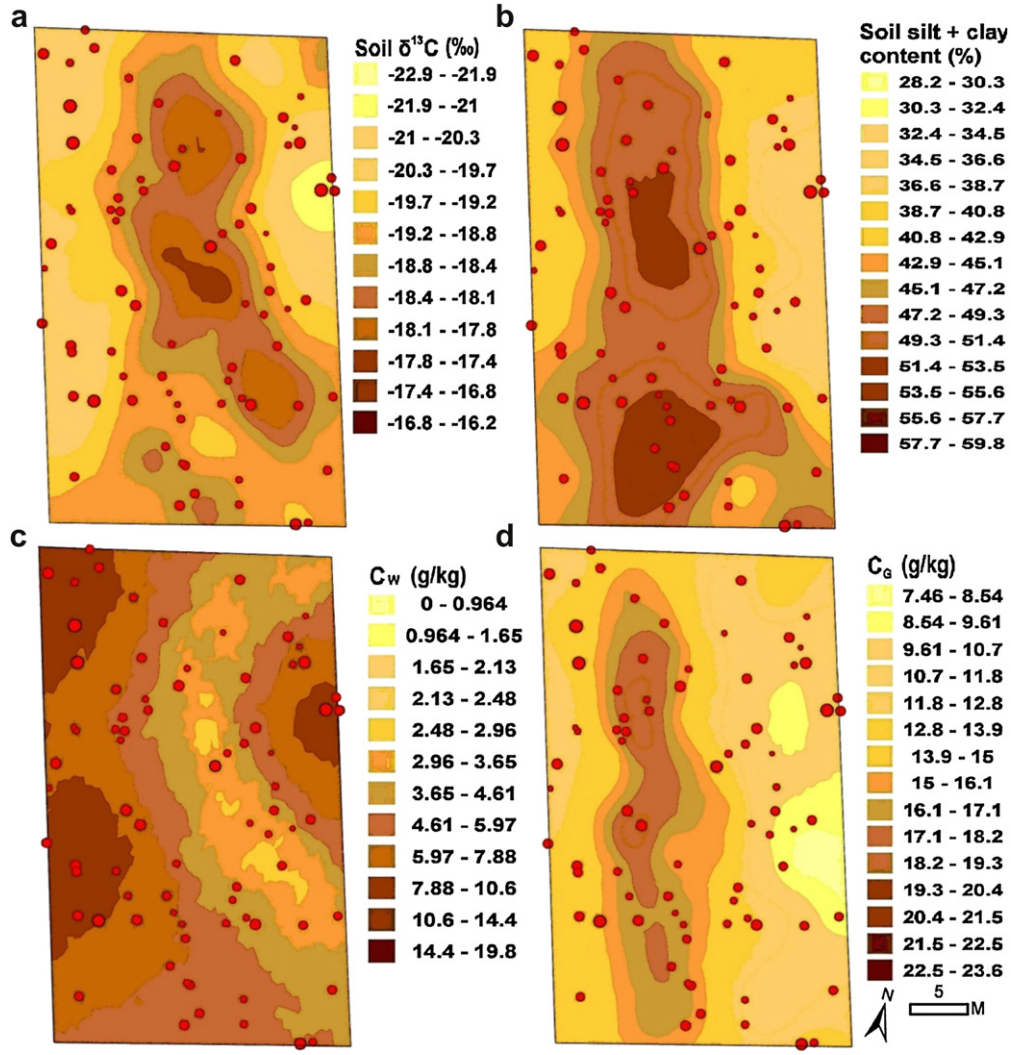

Fig. 2. Kriged maps of edaphic properties within a mesquite woodland (Fig. 1) occupying an intermittent drainage once dominated by C_4 grasses. Maps were developed from grid sample points only. (a) Soil $\delta^{13}C$ (‰), (b) soil silt + clay content (%), (c) SOC concentration derived from woody plants (C_W; g C kg^{-1}), and (d) SOC derived from previous grassland (C_G; g C kg^{-1}). Red dots denote mesquite trees; dot size is proportional to tree basal diameter. The intermittent drainage generally runs north-south with the topographic low generally occurring in the center of the image, with elevation gradually increasing to the east and west. (For interpretation of the references to color in this figure legend, the reader is referred to the web version of this article.)

primary production, (e) the biochemical composition of plant tissues, and (f) microbial activities and products (Boutton, 1996; Boutton et al., 1998; Marriott et al., 1997; Ehleringer et al., 2000; Biggs et al., 2002; Powers, 2006). These biological factors will also interact with abiotic environmental characteristics (including soil texture, hydrologic setting, and soil microclimate) to influence the spatial pattern of soil $\delta^{13}C$ values that develops across a landscape (van Kessel et al., 1994; Bird et al., 2004; Bai et al., 2009). As

Table 4
Pearson product–moment correlation coefficients (r) showing relationships between soil $\delta^{13}C$, GPI (conspecific species influence index), SOC, root biomass, and soil particle size distribution. C_G = SOC derived from previous grassland while C_W = SOC derived from new woody input. All the sample points in the grids and transects are included ($n = 207$). Significance of correlation coefficients was determined by modified t-tests that account for the effects of spatial autocorrelation (Clifford et al., 1989; Dutilleul et al., 1993).

	GPI	SOC (g C kg^{-1})	C_W (g C kg^{-1})	C_G (g C kg^{-1})	Root (g m^{-2})	Sand (%)	Silt (%)	Clay (%)	Silt + Clay (%)
$\delta^{13}C$	−0.12	−0.63**	−0.92**	0.23*	−0.48**	−0.41**	0.22*	0.41**	0.41**
GPI		0.23*	0.21*	0.17	0.10	−0.13	0.26**	0.02	0.13
SOC			0.77**	0.60**	0.49**	−0.29**	0.29**	0.21*	0.29**
C_W					0.53**	0.19	−0.11	−0.19	−0.19
C_G					0.15	−0.78**	0.60**	0.66**	0.78**
Root						0.05	0.01	−0.06	−0.05
Sand							−0.68**	−0.91**	1.00**
Silt								0.30**	0.68**
Clay									0.91**

**$p < 0.01$.
*$p < 0.05$.

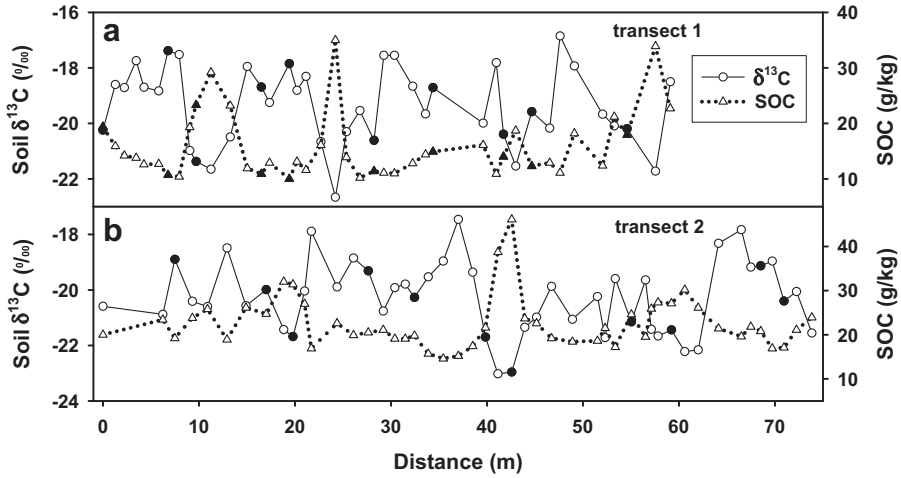

Fig. 3. Soil $\delta^{13}C$ (‰) and SOC (g kg^{-1}) along tree-to-tree transects T1 (a) and T2 (b). Values along *X*-axes are the actual distances (m). Circles and solid line represent soil $\delta^{13}C$; triangles and dotted line represent SOC. Solid black symbols indicate points adjacent to mesquite tree trunks. For comparison, the $\delta^{13}C$ surface litter and leaves of mesquite are −28 to −26‰ and −26 to −25‰, respectively (Boutton et al., 1998; Bai et al., 2008).

summarized in the following sections, our data suggest that strong interactions between hydrology, plant community characteristics, SOC, and soil texture are at play.

4.2. Soil $\delta^{13}C$ and plant community characteristics

Previous studies at this site have indicated that woody plant encroachment into grasslands was initiated by the establishment of honey mesquite within the grassland matrix in the late 1800s/early 1900s. As these colonizing mesquite trees established and grew, they served as recruitment foci, facilitating the recruitment and establishment of other woody species beneath their canopies (Archer et al., 1988; Archer, 1995). $\delta^{13}C$ values support this pattern of succession in the uplands - values are lowest in the centers of woody clusters near the base of the founding mesquite tree, and increase continuously along transects into the surrounding grassland (Millard et al., 2008; Bai et al., 2009). Therefore, we expected that the spatial pattern of soil $\delta^{13}C$ in lowland woodlands would also be related to the distribution of mesquite trees. However, proximity of soil samples to mesquite trees (as quantified by the GPI) was not significantly correlated with soil $\delta^{13}C$ (Table 4). Similarly, there was no significant difference between the $\delta^{13}C$ values of soils adjacent to mesquite tree trunks vs. those at the edge of their canopies along the two transects (Table 2).

One potential explanation for this result is that these lower-lying woodlands are significantly older than the woody clusters and groves in the uplands, and carbon isotopic evidence for the role of mesquite in woody invasion into the lowlands has either decayed out of the system or become less distinct due to organic matter inputs from understory shrubs. However, this seems unlikely as the age distribution of mesquite trees in lowlands is generally similar to that of mesquite trees in the uplands (Boutton et al., 1998). Another possibility is that periodic flooding of these low-lying portions of the landscape (Scifres and Mutz, 1975; Farley et al., 2010) could have redistributed shrub litter and sediments and obscured the time signal that might otherwise be present in the spatial data. However, recent studies have shown that SOC is derived primarily from roots, and that aboveground litter inputs have relatively little influence on SOC pools (Rasse et al., 2005; Garten, 2009; Kratterer et al., 2011). Furthermore, since the litter C pool size is very small relative to SOC (Boutton et al., 2009a), its periodic redistribution by infrequent flooding would probably have little effect on either the pool size or isotopic composition of SOC. Thus, if water redistribution is a factor, it may most likely be related to more to sediments than plant litter.

Alternatively, it is possible that grassland-to-woodland succession in the lowlands is not predicated on mesquite establishment as it is in the uplands (Archer et al., 1988), and instead, has occurred by a fundamentally different mechanism (e.g., water dispersal of seeds

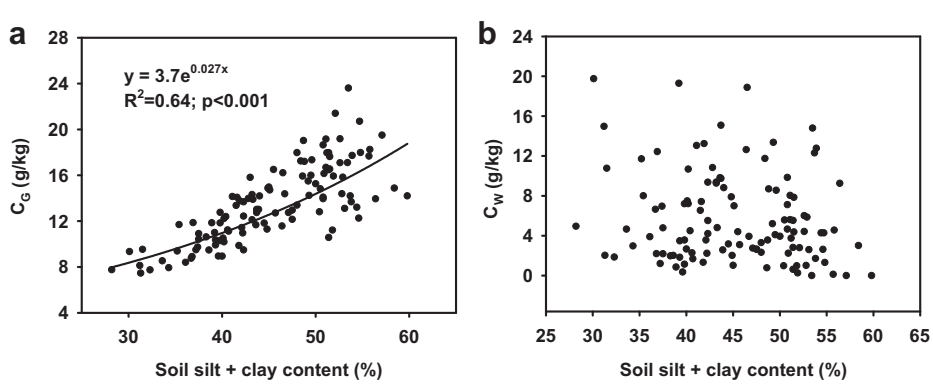

Fig. 4. Effect of soil silt + clay content (%) on SOC (g kg^{-1}) derived from C_4 grassland (a) compared to that derived from C_3 woodland (b). C_G = SOC derived from previous grassland while C_W = SOC derived from new woody input. All sample points from both the grids and transects are included (n = 207).

of mesquite and other C_3 shrubs) may have promoted simultaneous [as opposed to sequential] colonization of the C_4 grasslands that once dominated these lowland portions of the landscape. Given that potentially limiting resources such as water, nitrogen, and phosphorus are more available in lowlands (McCulley et al., 2004; Wu and Archer, 2005; Bai et al., 2008; Boutton et al., 2009b), mesquite establishment may not be required to facilitate the establishment of other woody species on this portion of the landscape as it is in uplands. In this hypothesized scenario, C_3 shrub root and litter inputs would have been relatively ubiquitous and not concentrated under mesquite canopies.

4.3. Soil $\delta^{13}C$ and SOC concentration

SOC is controlled by the balance of C input from plant biomass and output through decomposition (Jenny, 1941; Schlesinger, 1977). Increases in SOC can be a result of more C input, lower decomposition rates or a combination of the two. In areas with woody invasion, changes in amount of litter input, tissue chemical composition and root biomass accompanying the development of the woody patches may have significant influences on SOC. We found a positive correlation between SOC concentration and root biomass density ($r = 0.49$, Table 4) and a negative correlation between soil $\delta^{13}C$ and root biomass ($r = -0.48$, Table 4), both suggesting root carbon inputs are important determinants of SOC at this site. This is consistent with the review by Rasse et al. (2005), showing that most SOC is derived from roots rather than aboveground litter inputs. The negative correlation between soil $\delta^{13}C$ and SOC indicated that C_3 woody carbon instead of original grassland carbon was mainly the cause of higher SOC concentration. These results indicate that woody plant encroachment has caused higher root biomass density and higher SOC concentration in this area, consistent with previous studies (Connin et al., 1997; McPherson, 1997; Scholes and Archer, 1997; Hibbard et al., 2001; Liao et al., 2006b). Furthermore, the new SOC pool (C_W) was positively correlated with root biomass, whereas the old SOC pool (C_G) was positively correlated with silt + clay. This suggests recent carbon inputs (roots) control the C_W pool, whereas texture (silt + clay) controls C_G pool through its influence on decomposition rate.

SOC, soil $\delta^{13}C$ and soil silt + clay content exhibited comparable spatial autocorrelation ranges (15.6–18.2 m; Table 3). We can only speculate about what might cause variation in these variables at this scale. One hypothesis: coarse woody debris from large shrubs determines the spatial structure of these variables by influencing how water redistributes litter and sediments. The weaker spatial structure of C_W ($Sill_{(SD)} = 31.7\%$; Table 3) suggests newer woody carbon inputs have been delivered to the soil in a relatively homogenous fashion across this woodland landscape characterized by a high density of shrubs beneath and between mesquite overstory canopies. This is consistent with the GPI analysis showing that soil $\delta^{13}C$ values were not significantly affected by the size, abundance or proximity to mesquite trees. It is noteworthy that C_W and root biomass had a strong spatial structure ($Sill_{(SD)} = 83.4\%$), but the range over which root biomass was correlated with C_W was relatively small, and beyond this distance (7.1 m), it no longer influenced C_W (Table 3). We speculate that spatial patterns of root carbon input to the SOC pool are related to the distribution of the near-surface primary, coarse lateral roots that produce the small roots captured in shallow (0–15 cm) soil cores.

4.4. Soil $\delta^{13}C$ and soil texture

The mean of all soil $\delta^{13}C$ values in this woodland was −19.5‰, which was higher than values obtained previously in upland woody patches (approximately −22‰) (Boutton et al., 2009a). Liao et al. (2006a) also found soil $\delta^{13}C$ values of drainage woodlands were higher than those of upland woody patches, and suggested that higher soil silt + clay content in the drainage woodlands may be responsible for this observation. Fine mineral particles are critical for the formation of organomineral complexes and microaggregates, which stabilize soil organic matter physically and protect it from decay (Jastrow and Miller, 1998; Six et al., 2002). The positive correlation between soil silt + clay content and $\delta^{13}C$ values (Table 4) suggests grassland-derived C_4 SOC would persist longer and thus inflate soil $\delta^{13}C$ values relative to that in sandier upland soils.

Spatial variation in soil texture can be manifest at plant to landscape to regional scales (e.g., Davidson, 1995; Hirobe et al., 2001; Shahandeh et al., 2005; Su et al., 2006). In our intermittent drainage landscape, the range of spatial autocorrelation in soil texture (silt + clay content) was 16.2 m and it influenced soil $\delta^{13}C$ over a range of 16.5 m (Table 3). In contrast, soil texture varied little in the adjoining upland landscape at this site and hence was not a factor in spatial patterns of soil $\delta^{13}C$ (Bai et al., 2009). It is interesting to note that while soil texture emerged as having strong influence on the spatial structure carbon remaining from past grasslands ($Sill_{(HD)} = 85.7\%$; cross-variogram portion of Table 3), it did not emerge as a factor influencing the spatial structure of the more recent shrub-derived soil carbon. These results suggests litter inputs (roots in this instance) are main determinants of spatial structure of SOC dynamics in the short-term in these intermittent drainage woodlands; but that over the long-term soil carbon pool dynamics are governed by soil physical properties affording long-term protection of soil organic matter (Anderson and Paul, 1984; Ladd et al., 1985; Hassink, 1997; Zinn et al., 2005; Liao et al., 2006a) and the behavior of recalcitrant organic matter constituents.

As a general test of this inference, we estimated the effect of soil texture on soil organic carbon decomposition rates. Assuming there would have been little fresh C_4 carbon input into the system after the vegetation change, changes in grassland carbon (C_G) would be mainly controlled by decomposition processes. According to first order kinetics, $C_G = C_0 \times e^{-kt}$, where C_0 is the SOC concentration at the time of vegetation change ($t = 0$), t is the time-step, and k is the fractional rate constant for SOC decay. We found C_G was a significant exponential function of silt + clay content: $C_G = 3.7 \times e^{0.027x}$ where x = silt + clay (Fig. 4a, $r^2 = 0.64$; $p < 0.001$). Therefore, by combining and rearranging these two equations, we find $k = (\ln C_0 - \ln 3.7 - 0.027x)/t$, which indicates the fractional rate constant k has a negative linear relationship with soil silt + clay content (x). This result supports the linear relationship between soil texture and k used in modeling (Hansen et al., 1990; Parton et al., 1994; Bosatta and Ågren, 1997). Soil silt + clay content were not correlated with new woody carbon input though (Fig. 4b), which suggested the new carbon was not yet associated with physical protection mechanisms related to silt + clay.

Utilizing the mean values for soil properties in Table 1 ($C_0 = 19.3$ g C/kg soil; x = silt + clay = 43.6%) and assuming t is equal to the average age of the mesquite trees in the drainage woodlands (48.8 years; Boutton et al., 1998), then the equation in the previous paragraph yields an average k-value for SOC of 0.0098/yr. This value is within the range of those obtained using natural ^{13}C ($k = 0.0087$/yr) and natural ^{14}C ($k = 0.018$/yr) kinetics in drainage woodlands at this same site (Boutton et al., 2009a). And, an average k-value of 0.0098/yr is at the lower end of the range reported from other grassland and forest ecosystems around the world (0.001–0.045/yr, Six and Jastrow, 2002).

5. Conclusion

Soil particle size distribution played an important role in determining spatial patterns of soil $\delta^{13}C$ in this subtropical

woodland where C_3 trees and shrubs have replaced communities dominated by C_4 grasses during the past century. Prior studies in upland portions of this landscape indicate that the transition from grassland-to-woodland is initiated by colonization of mesquite trees in the grassland matrix, with the location of mesquite trees exerting strong control over spatial patterns of SOC and soil $\delta^{13}C$. However, spatial patterns of soil $\delta^{13}C$ in this lowland woodland were not related to the locations of mesquite trees, suggesting that (a) these overstory trees no longer govern SOC storage and dynamics, (b) periodic flooding of these intermittent drainage landforms has redistributed shrub litter and surface soils and obscured the mesquite signal that might otherwise be present in the spatial data, and/or (c) the mechanisms of grassland-to-woodland succession are fundamentally different in the lowland woodlands than they are in the uplands. Instead, spatial patterns of soil $\delta^{13}C$ in these lower-lying woodlands co-varied with soil texture and SOC pool sizes. The negative correlation between SOC concentration and soil $\delta^{13}C$ indicated that on those portions of the landscape with high SOC, a significant proportion of that SOC was derived from the invading C_3 woody plants.

Elucidation of the spatial structure of variables related soil carbon cycling provided new perspectives to guide future research. For example, observations that root biomass was spatially correlated with new SOC from woody plants within a distances of 7.1 m, whereas soil texture controlled soil $\delta^{13}C$ and decomposition of old SOC from grassland over ranges of 16–23 m challenge us to identify what earth system processes and ecosystem structures might be driving carbon cycling at these contrasting scales. Improvements in our understanding how controls over soil carbon cycling change with spatial scale will enhance our ability to design vegetation and soil sampling regimes; and to use soil $\delta^{13}C$ as a tool to infer vegetation and soil organic carbon dynamics in ecosystems where C_3–C_4 transitions and changes in structure and function are occurring.

Acknowledgments

This work was supported by the NSF Ecosystem Studies Program grant DEB-9981723. Additional support was provided by the Key Program of the Chinese Academy of Sciences Project KZCX2-YW-BR-20 to E.B. and Regents and Tom Slick Fellowships from Texas A&M University to E.B. and F.L. We are grateful to Kirk Jessup, Lisa Alexander, Donna Prochaska, Terri Rosol, Andrew Boutton, and Heather Jahnsen for assistance with field work and laboratory analyses. We thank Dr. Fred Smeins whose constructive comments helped improve the manuscript. Thanks are also extended to David McKown, manager of the La Copita Research Area, for assistance with on-site logistics. Finally, the authors would also like to thank two anonymous reviewers for their helpful comments on earlier drafts of this article.

References

Agren, G.I., Bosatta, E., Balesdent, J., 1996. Isotope discrimination during decomposition of organic matter: a theoretical analysis. Soil Science Society of America Journal 60, 1121–1126.

Amundson, R., Stern, L., Baisden, T., Wang, Y., 1998. The isotopic composition of soil and soil-respired CO_2. Geoderma 82, 83–114.

Anderson, D.W., Paul, E.A., 1984. Organo-mineral complexes and their study by radiocarbon dating. Soil Science Society of America Journal 48, 298–301.

Archer, S., Scifres, C., Bassham, C.R., Maggio, R., 1988. Autogenic succession in a subtropical savanna: conversion of grassland to thorn woodland. Ecological Monographs 58, 111–127.

Archer, S., Boutton, T.W., Hibbard, K.A., 2001. Trees in Grasslands: Biogeochemical Consequences of Woody Plant Expansion. In: E-Schulze, D., Heimann, M., Harrison, S.P., Holland, E.A., Lloyd, J., Prentice, I.C., Schimel, D. (Eds.), Global Biogeochemical Cycles in the Climate System. Academic Press, San Diego, CA, USA, pp. 115–138.

Archer, S., 1995. Tree-grass dynamics in a *Prosopis*-thorn scrub savanna parkland: reconstructing the past and predicting the future. Ecoscience 2, 83–89.

Bai, E., Boutton, T., Liu, F., Wu, X., Archer, S., 2008. Variation in woody plant $\delta^{13}C$ along a topoedaphic gradient in a subtropical savanna parkland. Oecologia 156, 479–489.

Bai, E., Boutton, T.W., Wu, X.B., Liu, F., Archer, S.R., 2009. Landscape-scale vegetation dynamics inferred from spatial patterns of soil $\delta^{13}C$ in a subtropical savanna parkland. Journal of Geophysical Research 114, G01019. doi:10.1029/02008JG000839.

Balesdent, J., Mariotti, A., 1996. Measurement of soil organic matter turnover using ^{13}C natural abundance. In: Boutton, T.W., Yamasaki, S.I. (Eds.), Mass Spectrometry of Soils. Marcel Dekker Inc., New York.

Balesdent, J., Mariotti, A., Guillet, B., 1987. Natural 13C abundance as a tracer for studies of soil organic matter dynamics. Soil Biology and Biochemistry 19, 25–30.

Biggs, T.H., Quade, J., Webb, R.H., 2002. $\delta^{13}C$ values of soil organic matter in semiarid grassland with mesquite (*Prosopis*) encroachment in southeastern Arizona. Geoderma 110, 109–130.

Bird, M., Kracht, O., Derrien, D., Zhou, Y., 2003. The effect of soil texture and roots on the stable carbon isotope composition of soil organic carbon. Australian Journal of Soil Research 41, 77–94.

Bird, M.I., Veenendaal, E.M., Lloyd, J.J., 2004. Soil carbon inventories and $\delta^{13}C$ along a moisture gradient in Botswana. Global Change Biology 10, 342–349.

Blair, N., Leu, A., Munoz, E., Olsen, J., Kwong, E., Des Marais, D., 1985. Carbon isotopic fractionation in heterotrophic microbial metabolism. Applied and Environmental Microbiology 50, 996–1001.

Boeckx, P., Van Meirvenne, M., Raulo, F., Van Cleemput, O., 2006. Spatial patterns of $\delta^{13}C$ and $\delta^{15}N$ in the urban topsoil of Gent, Belgium. Organic Geochemistry 37, 1383–1393.

Bosatta, E., Ågren, G.I., 1997. Theoretical analyses of soil texture effects on organic matter dynamics. Soil Biology and Biochemistry 29, 1633–1638.

Boutton, T.W., Archer, S.R., Midwood, A.J., Zitzer, S.F., Bol, R., 1998. $\delta^{13}C$ values of soil organic carbon and their use in documenting vegetation change in a subtropical savanna ecosystem. Geoderma 82, 5–41.

Boutton, T.W., Archer, S.R., Midwood, A.J., 1999. Stable isotopes in ecosystem science: structure, function and dynamics of a subtropical Savanna. Rapid Communications in Mass Spectrometry 13, 1263–1277.

Boutton, T.W., Liao, J.D., Filley, T.R., Archer, S.R., 2009a. Belowground carbon storage and dynamics accompanying woody plant encroachment in a subtropical savanna. In: Lal, R., Follett, R. (Eds.), Soil Carbon Sequestration and the Greenhouse Effect. Soil Science Society of America, Madison, WI, pp. 181–205.

Boutton, T.W., Kantola, I.B., Stott, D.E., Balthrop, S.L., Tribble, J.E., Filley, T.R., 2009b. Soil phosphatase activity and plant available phosphorus increase following grassland invasion by N-fixing tree legumes. Eos, Transactions of the American Geophysical Union 90 B21B–0338.

Boutton, T.W., 1996. Stable carbon isotope ratios of soil organic matter and their use as indicators of vegetation and climate change. In: Boutton, T.W., Yamasaki, S.I. (Eds.), Mass Spectrometry of Soils. Marcel Dekker, Inc., New York, New York, USA, pp. 47–82.

Brown, A.J., 1999. Soil sampling and sample handling for chemical analysis. In: Peverill, K.I., Sparrow, L.A., Reuter, D.J. (Eds.), Soil Analysis: An Interpretation Manual. CSIRO, Collingwood, Australia, pp. 35–53.

Choi, Y., Wang, Y., Hsieh, Y.P., Robinson, L., 2001. Vegetation succession and carbon sequestration in a coastal wetland in northwest Florida: evidence from carbon isotopes. Global Biogeochemical Cycles 15, 311–319.

Clifford, P., Richardson, S., Hemon, D., 1989. Assessing the significance of the correlation between two spatial processes. Biometrics 45, 123–134.

Connin, S.L., Virginia, R.A., Chamberlain, C.P., 1997. Carbon isotopes reveal soil organic matter dynamics following arid land shrub expansion. Oecologia 110, 374–386.

Coplen, T.B., 1996. New guidelines for reporting stable hydrogen, carbon, and oxygen isotope-ratio data. Geochimica et Cosmochimica Acta 60, 3359–3360.

Crow, S.E., Sulzman, E.W., Rugh, W.D., Bowden, R.D., Lajtha, K., 2006. Isotopic analysis of respired CO_2 during decomposition of separated soil organic matter pools. Soil Biology and Biochemistry 38, 3279–3291.

Davidson, E.A., 1995. Spatial covariation of soil organic carbon, clay content, and drainage class at a regional scale. Landscape Ecology 10, 349–362.

Desjardins, T., Andreux, F., Volkoff, B., Cerri, C.C., 1994. Organic carbon and ^{13}C contents in soils and soil size-fractions, and their changes due to deforestation and pasture installation in eastern Amazonia. Geoderma 61, 103–118.

Diochon, A., Kellman, L., 2008. Natural abundance measurements of ^{13}C indicate increased deep soil carbon mineralization after forest disturbance. Geophysical Research Letters 35, L14402. doi:10.1029/2008GL034795.

Dümig, A., Schad, P., Rumpel, C., Dignac, M.-F., Kögel-Knabner, I., 2008. Araucaria forest expansion on grassland in the southern Brazilian highlands as revealed by 14C and δ13C studies. Geoderma 145, 143–157.

Dutilleul, P., Clifford, P., Richardson, S., Hemon, D., 1993. Modifying the t test for assessing the correlation between two spatial processes. Biometrics 49, 305–314.

Ehleringer, J.R., Buchmann, N., Flanagan, L.B., 2000. Carbon isotope ratios in belowground carbon cycle processes. Ecological Applications 10, 412–422.

ESRI, I., 1998. Working with Arcview Spatial Analyst. ESRI, Inc., Redlands, California, USA.

Farley, A.L., Owens, P.R., Libohova, Z., Wu, X.B., Wilding, L.P., Archer, S.R., 2010. Use of terrain attributes as a tool to explore the interaction of vertic soils and surface hydrology in South Texas play a wetland systems. Journal of Arid Environments 74, 1487–1493.
Farquhar, G.D., Ehleringer, J.R., Hubick, K.T., 1989. Carbon isotope discrimination and photosynthesis. Annual Review of Plant Physiology and Plant Molecular Biology 40, 503–537.
Feller, C., Beare, M.H., 1997. Physical control of soil organic matter dynamics in the tropics. Geoderma 79, 69–116.
Fernandez, I., Mahieu, N., Cadisch, G., 2003. Carbon isotopic fractionation during decomposition of plant materials of different quality. Global Biogeochemical Cycles 17, 1075. doi:10.1029/2001GB001834.
Garten, C.T., Cooper, L.W., Post, W.M., Hanson, P.J., 2000. Climate controls on forest soil C isotope ratios in the Southern Appalachian Mountains. Ecology 81, 1108–1119.
Garten, C.T., 2009. A disconnect between O horizon and mineral soil carbon – implications for soil C sequestration. Acta Oecologica 35, 218–226.
Gee, G.W., Bauder, J.W., 1986. Particle-size analysis. In: Klute, A. (Ed.), Methods of Soil Analysis, Part I: Physical and Mineralogical Methods. American Society of Agronomy, Inc. and Soil Science Society of America, Inc., Madison, Wisconsin, USA, pp. 383–411.
Ghazoul, J., Liston, K.A., Boyle, T.J.B., 1998. Disturbance-induced density-dependent seed set in *Shorea siamensis* (Dipterocarpaceae), a tropical forest tree. Journal of Ecology 86, 462–473.
Goovaerts, P., 1997. Geostatistics for Natural Resources Evaluation. Oxford University Press, New York.
Hansen, S., Jensen, H.E., Neilsen, N.E., Svendsen, H., 1990. DAISY: A Soil Plant System Model. Danish Simulation Model for Transformation and Transport of Energy and Matter in the Soil Plant Atmosphere System. The National Agency for Environmental Protection, Copenhagen, 369 pp.
Harris, D., Horwáth, W.R., van Kessel, C., 2001. Acid fumigation of soils to remove carbonates prior to total organic carbon or CARBON-13 isotopic analysis. Soil Science Society of America Journal 65, 1853–1856.
Hassink, J., 1997. The capacity of soils to preserve organic C and N by their association with clay and silt particles. Plant and Soil 191, 77–87.
Hibbard, K.A., Archer, S., Schimel, D.S., Valentine, D.W., 2001. Biogeochemical changes accompanying woody plant encroachment in a subtropical savanna. Ecology 82, 1999–2011.
Hirobe, M., Ohte, N., Karasawa, N., Zhang, G.-s., Wang, L.-h., Yoshikawa, K., 2001. Plant species effect on the spatial patterns of soil properties in the Mu-us desert ecosystem, Inner Mongolia, China. Plant and Soil 234, 195–205.
Jastrow, J.D., Miller, R.M., 1998. Soil aggregate stabilization and carbon sequestration: feedbacks through organomineral associations. In: Lal, R., Kimble, J.M., Follett, R.F., Stewart, B.A. (Eds.), Soil Processes and the Carbon Cycle. CRC Press, Boca Raton, FL, pp. 207–224.
Jenny, H., 1941. Factors of Soil Formation. McGraw-Hill, New York, New York, USA.
Jobbagy, E.G., Jackson, R.B., 2000. The vertical distribution of soil organic carbon and its relation to climate and vegetation. Ecological Applications 10, 423–436.
Kratterer, T., Bolinder, M.A., AndrÈn, O., Kirchmann, H., Menichetti, L., 2011. Roots contribute more to refractory soil organic matter than above-ground crop residues, as revealed by a long-term field experiment. Agriculture, Ecosystems & Environment 141, 184–192.
Krull, E.G., Skjemstad, J.O., Burrows, W.H., Bray, S.G., Wynn, J.G., Bol, R., Spouncer, L., Harms, B., 2005. Recent vegetation changes in central Queensland, Australia: evidence from $\delta^{13}C$ and ^{14}C analyses of soil organic matter. Geoderma 126, 241–259.
Krull, E., Bray, S., Harms, B., Baxter, N., Bol, R., Farquhar, G., 2007. Development of a stable isotope index to assess decadal-scale vegetation change and application to woodlands of the Burdekin catchment, Australia. Global Change Biology 13, 1455–1468.
Ladd, J.N., Amato, M., Oades, J.M., 1985. Decomposition of plant material in Australian soils. III. Residual organic and microbial biomass C and N from isotope-labeled legume material and soil organic matter, decomposing under field conditions. Australian Journal of Soil Research 23, 603–611.
Liao, J.D., Boutton, T.W., Jastrow, J.D., 2006a. Organic matter turnover in soil physical fractions following woody plant invasion of grassland: evidence from natural ^{13}C and ^{15}N. Soil Biology and Biochemistry 38, 3197–3210.
Liao, J.D., Boutton, T.W., Jastrow, J.D., 2006b. Storage and dynamics of carbon and nitrogen in soil physical fractions following woody plant invasion of grassland. Soil Biology and Biochemistry 38, 3184–3196.
Ludlow, M.M., Troughton, J., Jones, R., 1976. A technique for determining the proportion of C_3 and C_4 species in plant samples using stable natural isotopes of carbon. Journal of Agricultural Science 87, 625–632.
Marriott, C.A., Hudson, G., Hamilton, D., Neilson, R., Boag, B., Handley, L.L., Wishart, J., Scrimgeour, C.M., Robinson, D., 1997. Spatial variability of soil total C and N and their stable isotopes in an upland Scottish grassland. Plant and Soil 196, 151–162.
McCulley, R.L., Archer, S.R., Boutton, T.W., Hons, F.M., Zuberer, D.A., 2004. Soil respiration and nutrient cycling in wooded communities developing in grassland. Ecology 85, 2804–2817.
McPherson, G.R., 1997. Ecology and Management of North American Savannas. University of Arizona Press, Tucson, AZ.
Millard, P., Midwood, A.J., Hunt, J.E., Whitehead, D., Boutton, T.W., 2008. Partitioning soil surface CO_2 efflux into autotrophic and heterotrophic components, using natural gradients in soil $\delta^{13}C$ in an undisturbed savannah soil. Soil Biology and Biochemistry 40, 1575–1582.
Nadelhoffer, K.J., Fry, B., 1988. Controls on natural nitrogen-15 and carbon-13 abundances in forest soil organic matter. Soil Science Society of America Journal 52, 1633–1640.
Nissenbaum, A., Schallinger, K.M., 1974. The distribution of the stable carbon isotope ($^{13}C/^{12}C$) in fractions of soil organic matter. Geoderma 11, 137–145.
Pannatier, Y., 1996. VARIOWIN, Software for Spatial Data Analysis in 2D. Springer, New York, New York, USA.
Parton, W.J., Schimel, D.S., Ojima, D.S., Cole, C.V., 1994. A general model for soil organic matter dynamics: sensitivity to litter chemistry, texture and management. In: Bryant, R.B., Arnold, R.W. (Eds.), Quantitative Modeling of Soil Farming Processes. SSSA Special Publication, Madison, Wisconsin, USA, ASA, CSSA, and SSA, pp. 147–167.
Pataki, D.E., Ellsworth, D.S., Evans, R.D., Gonzalez-Meler, M., King, J., Leavitt, S.W., Lin, G.H., Matamala, R., Pendall, E., Siegwolf, R., Van Kessel, C., Ehleringer, J.R., 2003. Tracing changes in ecosystem function under elevated carbon dioxide conditions. Bioscience 53, 805–818.
Pataki, D.E., Lai, C.-T., Keeling, C.D., Ehleringer, J.R., 2007. Insights from stable isotopes on the role of terrestrial ecosystems in the global carbon cycle. In: Canadell, J.G., Pataki, D.E., Pitelka, L.F. (Eds.), Terrestrial Ecosystems in a Changing World, pp. 37–44.
Ping, X., Zhou, G., Zhuang, Q., Wang, Y., Zuo, W., Shi, G., Lin, X., Wang, Y., 2010. Effects of sample size and position from monolith and core methods on the estimation of total root biomass in a temperate grassland ecosystem in Inner Mongolia. Geoderma 155, 262–268.
Powers, J.,S., 2006. Spatial variation of soil organic carbon concentrations and stable isotopic composition in 1-ha plots of forest and pasture in Costa Rica: implications for the natural abundance technique. Biology and Fertility of Soils 42, 580–584.
Rasse, D., Rumpel, C., Dignac, M.-F., 2005. Is soil carbon mostly root carbon? Mechanisms for a specific stabilisation. Plant and Soil 269, 341–356.
Rosenberg, M.S., 2001. PASSAGE: pattern analysis, spatial statistics, and geographic exegesis. In: Department of Biology. Arizona State University, Tempe, Arizona, USA.
Rossi, J.P., Delaville, L., Quénéhervé, P., 1996. Microspatial structure of a plant-parasitic nematode community in a sugarcane field in Martinique. Applied Soil Ecology 3, 17–26.
Sanaiotti, T.M., Martinelli, L.A., Victoria, R.L., Trumbore, S.E., Camargo, P.B., 2002. Past vegetation changes in Amazon savannas determined using carbon isotopes of soil organic matter. Biotropica 34, 2–16.
Santruckova, H., Bird, M.I., Lloyd, J., 2000. Microbial processes and carbon-isotope fractionation in tropical and temperate grassland soils. Functional Ecology 14, 108–114.
Schimel, D.S., Holland, E.A., McKeown, R., 1994. Climatic, edaphic, and biotic controls over storage and turnover of carbon in soils. Global Biogeochemical Cycles 8, 279–293.
Schlesinger, W.H., 1977. Carbon balance in terrestrial detritus. Annual Review of Ecology and Systematics 8, 51–81.
Scholes, R.J., Archer, S.R., 1997. Tree-grass interactions in savannas. Annual Review of Ecology and Systematics 28, 517–544.
Scifres, C.J., Mutz, J.L., 1975. Secondary succession following extended inundation of Texas coastal rangeland. Journal of Range Management 28, 279–282.
Shahandeh, H., Wright, A.L., Hons, F.M., Lascano, R.J., 2005. Spatial and temporal variation of soil nitrogen parameters related to soil texture and corn yield. Agronomy Journal 97, 772–782.
Silva, L.C.R., Sternberg, L., Haridasan, M., Hoffmann, W.A., Miralles-Wilhelm, F., Franco, A.C., 2008. Expansion of gallery forests into central Brazilian savannas. Global Change Biology 14, 2108–2118.
Six, J., Jastrow, J.D., 2002. Organic matter turnover. In: Encyclopedia of Soil Science. Marcel Dekker, New York, pp. 936–942.
Six, J., Conant, R.T., Paul, E.A., Paustian, K., 2002. Stabilization mechanisms of soil organic matter: implications for C-saturation of soils. Plant and Soil 241, 155–176.
Smucker, A.J.M., McBurney, S.L., Srivanstava, A.K., 1982. Quantitative separation of roots from compacted soil profiles by the hydropneumatic elutriation system. Agronomy Journal 74, 500–503.
Soil Survey Staff, 1996. Soil survey laboratory methods manual. In: Soil Survey Investigations Report. USDA-NRCS, Lincoln, NE.
SpaceStat, TerraSeer Inc, 2000. Ann Arbor, MI. Version 2.0.27.
SPSS Inc., 2002. Chicago, IL. SPSS for Windows, Version 11.5.
Su, Y.Z., Li, Y.L., Zhao, H.L., 2006. Soil properties and their spatial pattern in a degraded sandy grassland under post-grazing restoration, Inner Mongolia, northern China. Biogeochemistry 79, 297–314.
Suits, N.S., Denning, A.S., Berry, J.A., Still, C.J., Kaduk, J., Miller, J.B., Baker, I.T., 2005. Simulation of carbon isotope discrimination of the terrestrial biosphere. Global Biogeochemical Cycles 19, GB1017. doi:10.1029/2003GB002141.
Troughton, J.H., Stout, J.D., Rafter, T.A., 1974. Long-term Stability of Plant Communities. Carnegie Inst Wash Yearbook, pp. 838–845.
van Kessel, C., Farrell, R.E., Pennock, D.J., 1994. Carbon-13 and nitrogen-15 natural abundance in crop residues and soil organic matter. Soil Science Society of America Journal 58, 382–389.
West, J.B., Bowen, G.J., Dawson, T.E., Tu, K.P., 2010. Isoscapes: Understanding Movement, Pattern, and Process on Earth Through Isotope Mapping. Springer, New York, NY.
Wittmer, M.H.O.M., Auerswald, K., Bai, Y.F., Schäufele, R., Männel, T.T., Schnyder, H., 2009. Changes in the abundance of C3/C4 species of Inner Mongolia grassland:

evidence from isotopic composition of soil and vegetation. Global Change Biology 16, 605–616.
Wu, X., Archer, S., 2005. Scale-dependent influence of topography-based hydrologic features on patterns of woody plant encroachment in savanna landscapes. Landscape Ecology 20, 733–742.
Wynn, J.G., Bird, M.I., 2007. C_4-derived soil organic carbon decomposes faster than its C_3 counterpart in mixed C_3/C_4 soils. Global Change Biology 13, 2206–2217.
Zinn, Y.L., Lal, R., Resck, D.V.S., 2005. Texture and organic carbon relations described by a profile pedotransfer function for Brazilian Cerrado soils. Geoderma 127, 168–173.